Journal Name

Dynamic Article Links ►

Cite this: DOI: 10.1039/c0xx00000x

www.rsc.org/xxxxxx

ARTICLE TYPE

SnO-Nanocluster Modified Anatase TiO2 Photocatalyst: Exploiting the Sn(II) Lone Pair for a new Photocatalyst Material with Visible Light Absorption and Charge Carrier Separation

Anna Iwaszuk and Michael Nolan

Received (in XXX, XXX) Xth XXXXXXXXX 200X, Accepted Xth XXXXXXXXX 200X
First published on the web Xth XXXXXXXXX 200X
DOI: 10.1039/

Abstract Modifying TiO_2 to design new photocatalysts with visible light absorption and reduced charge carrier recombination for photocatalytic depollution or water splitting is a very active field. A promising approach is to deposit small nanoclusters of a metal oxide on a semiconducting oxide such as TiO_2 or $ZnGa_2O_4$. In this paper we present a first principles density functional theory (DFT) investigation of a novel concept in photocatalyst materials design: Sn(II)O nanoclusters supported on TiO_2 anatase (001) and demonstrate that the presence of the Sn(II)-O lone pair in the nanoclusters gives a new approach to engineering key properties for photocatalysis. The modification of anatase with Sn(II)O reduces the band gap over unmodified anatase, thus activating the material to visible light. This arises from the upwards shift of the valence band, due to the presence of the Sn 5s-O 2p lone pair in the nanocluster. Enhanced charge separation, which is key for photocatalytic efficiency, arises from the separation of electrons and holes onto the anatase surface and the Sn(II)O nanocluster. This work realises a new strategy of exploiting the lone pair in elements such as Sn to raise the VB edge of modified TiO_2 and enhance charge separation in new photocatalyst materials.

1. Introduction

TiO_2-based photocatalysis garners a significant amount of attention due to the potential for use in solar driven depollution of toxic organic pollutants from the domestic use and industrial activity [1-3] and water-splitting for environmentally friendly solar-hydrogen production to support the future hydrogen economy [4,5]. Among other useful properties it has a relatively low cost, good availability and non-toxicity. However despite presenting many outstanding features for the above applications, the wide band gap of TiO_2 allows light absorption only in UV region which is driving significant activity in so-called band gap engineering to enable visible light driven photocatalytic applications [6,7].

There have been many efforts to modify TiO_2 to reduce its band gap and enable visible light absorption; primarily using substitution of metal cations and/or non-metal anions at Ti and O sites of TiO_2 [8-14] and in recent years a co-doping approach, in which charge compensated dopants are used, has been advocated[15-17]. It is generally accepted that substituting a foreign atom onto the Ti or O site leads to the introduction of new states in the band gap of TiO_2 and this reduces the energy required for electronic transitions compared to unmodified TiO_2. This doping approach has shown some promising results, e.g. for N-doped TiO_2[18,19]. where the reduction in the band gap makes doped TiO_2 active in the visible light region and co-doping with C and Mo has been demonstrated [16]. On the other hand, it has been shown that while Cr-doping will reduce the band gap, it kills photocatalytic activity[20] and this issue arises from the localised nature of dopant derived electronic states that serve as recombination centres. However, practical problems such as stability, reproducibility and solubility also need to be addressed for achieving practical visible light active photocatalysts.

A newer approach is synthesising heterostructures composed of two different structures, with an intimate interface, which can improve both visible light absorption and charge carrier separation. Research in this area has shown that these new heterostructures can improve photocatalytic activities enhancing light absorption into visible region [21-24] and interesting examples include $BiVO_4$-WO_3,[25] AgI-BiO [26], BiOBr-$ZnFe_2O_4$,[27]. Furthermore these structures promote electron/hole separation upon photoexcitation.

More recently, an exciting approach is to fabricate heterostructures of TiO_2 modified by small, dispersed metal oxide nanoclusters, which has been demonstrated for FeO_x-modified TiO_2 by Libera[24] et al (atomic layer deposition,

ALD) and Tada [28-30] et al (chemisorption-calcination-cycling, CCC). Both approaches to synthesising the same surface modification showed a band gap reduction into the visible region, which was explained with density functional theory (DFT) simulations by the presence of FeO_x clusters at the valence band of TiO_2 [23,24,28]. Moreover the results of photoluminescence spectroscopy revealed a reduction in electron/hole recombination as evidenced by suppression of the PL signal of TiO_2 that is present at 540nm [28].

In modifying TiO_2 with metal oxide nanoclusters, we have also found that contrary to the results described above, the modification of TiO_2 with SnO_2 (Sn(IV) oxidation state) can give small enhancements in the visible region and strong UV activities for rutile TiO_2, but on anatase, only UV activity is displayed[30]. Analysis of the electronic structure in experiment and with density functional theory (DFT) highlights differences between the two forms of TiO_2. [22,30] Recent research shows that the oxidation state of the metal oxide deposited on TiO_2 can be important, with a recent example of $ZnGa_2O_4$ modification with SnO_2 and SnO [31] giving very different results. With an Sn^{2+} oxidation state visible light absorption is found, but not with Sn^{4+} oxidation state; the oxidation state of the tin oxide was controlled simply by the composition of the precursor, but the origin of this intriguing result was not discussed.

For these novel photocatalyst structures to be further applied, a detailed understanding of the role played by TiO_2 crystal form and oxidation state of the nanocluster modifier must be obtained, for which DFT simulations are useful in and in predicting novel heterostructures and rationalising experimental results

In light of the great potential of these novel heterostructured photocatalyst materials, we present in this paper a new strategy for modifying TiO_2 to achieve visible light absorption. The TiO_2 anatase (001) surface is modified by SnO clusters, with a 2+ Sn oxidation state, and this is shown to result in new heterostructures with visible light absorption and enhanced charge separation over unmodified anatase. We find a very strong effect due to tin oxidation state: the lone pair on the adsorbed tin oxide clusters results in the appearance of Sn-O derived states above the anatase valence band, narrowing the original anatase (001) band gap. A model of the photoexcited material reveals that improved charge carrier (electron and hole).separation Thus, we propose anatase TiO_2 modified with a lone-pair containing metal oxide as a novel visible light active photocatalytic material.

2. Methodology

To model TiO_2 anatase (001) surface, we use a three dimensional periodic slab model within the VASP code [32,33]. The valence electrons were described by a plane wave basis set and the cut-off for the kinetic energy is 396 eV. The number of valence electrons[34] is 4 for Ti, 4 for Sn and 6 for O. For both Ti [13] and Sn, testing with small core potentials shows little impact due to the choice of the core. The exchange-correlation functional was approximated by the Perdew-Wang 91 [35] functional. We use a Monkhorst-Pack (2×1×1) k-point sampling grid.

To describe Ti 3d states the DFT+U approach was used where U=4.5 eV. The need to introduce U parameter in order to describe properly electronic states of d shells is well known [36,37]. For Sn, the electronic states for both oxidation states are consistently described by DFT so no U correction is applied. The DFT+U approach gives a consistent description of the Ti 3*d* electrons states, but will still underestimate the band gap. While this is an important issue, we are primarily concerned with qualitative changes in the band gap upon surface modification, that is whether the metal oxide nanocluster reduces the energy gap or not and for this, DFT+U is sufficiently useful.

The unreconstructed model anatase (001) surface is studied, although a (1x4) reconstruction is observed experimentally under UHV[38]. The unreconstructed surface model used in this work is shown from other studies to be reasonable to describe this surface [39,40,41] and the (1x4) reconstruction displays similar oxygen species to those on the unreconstructed surface, so that the unreconstructed surface is a reasonable model for anatase (001) for this work. The outermost surface layer is terminated by two-fold coordinated oxygen atoms that bond with to 5-fold coordinated Ti atoms in the next atomic sublayer and in the next sublayer, the oxygen atoms are three-fold coordinated. A (4×2) surface supercell and 12 Å vacuum gap are used. The convergence criteria for the electronic and ionic relaxations are 0.0001 eV and 0.02 eV/ Å. For the consistency in the calculation we also applied the same supercell and technical parameters for the bare TiO_2 surface and free clusters.

The clusters are positioned on the TiO_2 surfaces and adsorption energy is computed from:

$$E\text{ads} = E((\text{SnO})\text{-}TiO_2) - \{ E(\text{SnO}) + E(TiO_2) \} \quad (1)$$

Where $E((\text{SnO})\text{-}TiO_2)$ is the total energy of the SnO cluster supported on the anatase surface and $E(\text{SnO})$ and $E(TiO_2)$ are the total energies of the free SnO cluster and the unmodified anatase surface. A negative adsorption energy indicates that cluster adsorption is stable.

To study a model of the photoexcited electronic state of SnO-modified anatase, we take the $(SnO)_4$-anatase model. In this model imposing a triplet electronic state puts an electron into the conduction band and leaves a valence band hole by construction. Therefore we model only the DFT ground state triplet and use this model to study the localisation of the photoexcited electron and hole and to examine the energies associated with trapping of the electron and hole. To describe the reduced Ti^{3+} formed in this model, we continue to use DFT+*U* (*U* = 4.5 eV on the Ti 3*d* states). To consistently describe the localized hole, the DFT+*U* approach is also applied to the O 2*p* states[42], with U = 5.5 eV[43-45]. The following calculations are performed:

a single point energy of the triplet at the singlet geometry, with an energy $E^{unrelaxed}$

a full ionic relaxation in the triplet electronic configuration, with an energy $E^{relaxed}$.

A dipole correction perpendicular to the surface plane is added to the total energies. Within this model we do not calculate energies that correspond to the energies obtained

from optical absorption, which would require TDDFT to describe the open shell singlet that results from electronic excitation. The following energies are calculated for bare anatase (001) and SnO-modified anatase (001):

(1) The singlet-triplet vertical unrelaxed energy: $E^{vertical} = E^{singlet} - E^{unrelaxed}$, where the singlet is fully relaxed and the triplet is not relaxed. This should correspond to the simple VB-CB energy gap from the density of states

(2) The singlet-triplet excitation energy: $E^{S-T} = E^{singlet} - E^{relaxed}$, where both the singlet and triplet electronic states are fully relaxed. The change in this energy with respect to the bare surface is a further means to determine the effect of the surface modification on the energy gap of TiO_2.

(3) The triplet relaxation (or trapping) energy: $E^{relax} = E^{relaxed} - E^{unrelaxed}$, where the first energy is the fully relaxed triplet and the second energy is the triplet state at the singlet geometry (single point calculation), so that E^{relax} is the energy gained when the electron and hole are trapped at their Ti and O sites upon structural relaxation.

3. Results

Figure 1 presents the relaxed atomic structures and adsorption energies for representative tin(II) oxide nanoclusters, SnO, Sn_2O_2, Sn_3O_3, Sn_4O_4, supported on the model anatase (001) surface. All clusters adsorb strongly at the surface, as evidenced by adsorption energies that are in the range from -2.92 eV to -5.71 eV and creating new interfacial metal-oxygen bonds. Table 1 presents details regarding the new metal-oxygen bonds between the clusters and the surface.

Regarding the adsorption energies, there are no clear trends, as can be expected from the properties of clusters at this length scale. However, the two larger clusters, $(SnO)_3$ and $(SnO)_4$ do show the strongest adsorption and comparison with the smaller nanoclusters suggests two possible influences on the adsorption energies. The first is that the adsorption of the smaller SnO and $(SnO)_2$ nanoclusters results in surface oxygen being pulled out of the anatase surface layer to form new interfacial bonds to Sn in the nanocluster, giving an Sn-O-Ti linkage; for SnO and $(SnO)_2$, two oxygens are pulled out of the surface layer. In the case of SnO one such oxygen is significantly pulled up, by 1 Å, when binding to Sn from the cluster and the second oxygen is pulled out of the surface by 0.6 Å. A similar situation is found for the adsorbed $(SnO)_2$, cluster with a displacement of O atoms by 1.0 Å and 0.5 Å. However, for $(SnO)_3$ and $(SnO)_4$, the surface O atoms are hardly displaced off their lattice sites. The adsorption energy of the nanoclusters is a balance between the energy gained by forming new nanocluster-surface bonds and any energy cost to distort the surface, e.g. the displacement of oxygen from the surface towards the nanocluster. Since the smaller clusters show significant migration of surface oxygen upon cluster adsorption, it is reasonable to propose that this leads to a smaller adsorption energy at the anatase (001) surface compared to the larger SnO nanoclusters. The second point is that the $(SnO)_4$ cluster is able to take an adsorption structure at this surface that is similar to that of bulk litharge structured SnO[46] and is well accommodated by the underlying anatase (001) surface, as can be seen in figure 1.

Examining the details of the atomic geometry, the adsorption of SnO and $(SnO)_2$ clusters results in formation of three new bonds with the distance between Sn in the nano cluster and surface oxygen being 2.31 Å in SnO and 2.11 Å and 2.15 Å in $(SnO)_2$ and for comparison the SnO litharge Sn-O distances are 2.26 Å, while the Sn-O distances in Sn_2TiO_4 are 2.09 and 2.21 Å[47] so the smaller SnO cluster has bonds in the same range as litharge. In both structures, the cluster oxygen to surface Ti distances are shorter than in bulk TiO_2, being 1.76 Å and 1.77 Å in SnO-anatase and 1.83 Å in $(SnO)_2$-anatase.

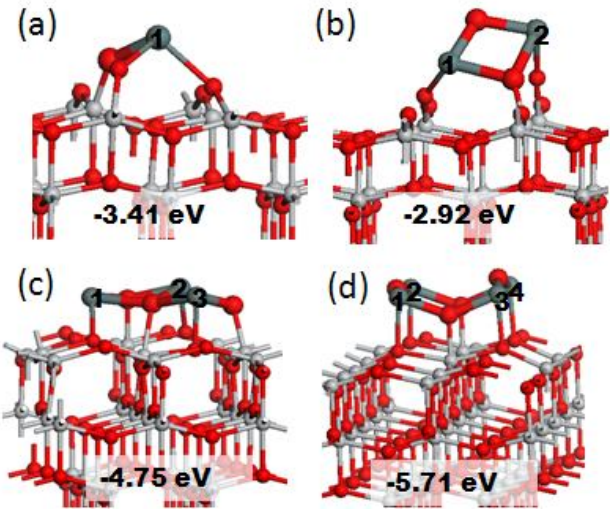

Fig1 Relaxed adsorption structures with adsorption energies given in eV for (a)SnO, (b)Sn_2O_2, (c)Sn_3O_3, (d)Sn_4O_4, clusters on TiO_2 anatase (001). The small grey sphere and red spheres are Ti and O from the surface. The large dark grey and red spheres are Sn and oxygen from the clusters. The Roman numerals shows the numbering of cluster configurations.

The two larger nanoclusters both create six new interfacial bonds with the anatase (001) surface. In both cases, Sn-surface O atoms distances are similar, being 2.15 Å – 2.22 Å for $(SnO)_3$ and 2.25 Å – 2.27 Å for $(SnO)_4$. So in this case the Sn-O bond lengths in $(SnO)_4$ are similar to litharge SnO. Cluster oxygen to surface-Ti distances are longer when compared to the smaller nanoclusters, being quite close to those of bulk TiO_2. We further compared the structures of the free and adsorbed SnO nanoclusters. For free $(SnO)_x$, nanoclusters the Sn-O bond lengths are in the range from 1.97 Å to 2.1 Å. The adsorbed $(SnO)_3$ cluster shows a significant change in the Sn-O bond lengths, which lie in the range of 2.12 Å to 2.37 Å while for $(SnO)_4$ we found four longer Sn-O bonds at 2.13 Å and four shorter Sn-O bonds in the range 1.99 Å and 2.00 Å. The Sn-O distances in the smaller adsorbed clusters are similar to the free clusters. In terms of free $(SnO)_3$ cluster structure which is like zigzag it tends to create a more closed structure while adsorbed on anatase (001). The free $(SnO)_4$ nanocluster has a ring structure (similar to ZnO nanoclusters of this size[48,49]) and maintains this shape while adsorbed on anatase (001).

Table 1: New surface-cluster Sn-O bond distances for SnO clusters absorbed on TiO_2 anatase (001).

[a] Sn from the cluster (Sn_c) and O from the surface (O_s).

[b] O from the cluster (O_c) and Ti from the surface (Ti_s)

	Distances / Å				
	Sn_c-O_s [(a)]	O_c-Ti_s [(b)]		Sn_c-O_s [(a)]	O_c-Ti_s [(b)]
SnO	2.31	1.77	Sn_3O_3	2.22 (1)	1.91
		1.76		2.17 (2)	2.18
				2.15 (3)	1.97
Sn_2O_2	2.15 (1)	1.83	Sn_4O_4	2.25 (1)	1.9
	2.11 (2)			2.26 (2)	1.9
				2.27 (3)	
				2.27 (4)	

3.2. Band Gap Changes Upon Modification of Anatase with SnO Nanoclusters

Figure 2 presents the electronic density of states projected (PEDOS) onto Sn 5*s* and O 2*p* states of the SnO clusters and Ti 3*d* and O 2*p* states of the anatase (001) surface. The PEDOS plots are used to investigate changes to the original TiO_2 anatase (001) valence-conduction band energy gap, which is determined to be 2.1 eV from DFT+U, as a result of interface formation in the heterostructure, and which generally proves to be a reliable guide to the effect of nanocluster modification on the energy gap of TiO_2.[22,23,30] From figure 2, we see that modification of anatase with SnO nanoclusters introduces new states into the original band gap of anatase (001), and that these states lie above the valence band edge of anatase. The presence of SnO derived states above the anatase valence band edge is particularly significant for the larger $(SnO)_3$ and $(SnO)_4$ nanoclusters and the consequence of this is *a narrowing of the original TiO_2 band gap by pushing the valence band edge up in energy*, while leaving the TiO_2 derived conduction band edge unchanged. The PEDOS plots suggest a shift in the VB edge of up to 1eV (for the $(SnO)_4$ nanocluster) from the original VB edge of TiO_2, which would result in visible light absorption. The unoccupied SnO states are found above the CB edge of TiO_2. The nature of the new states at the top of the VB can also be determined from the PEDOS and we see the influence of the SnO lone pair, with these states originating from Sn 5s and O 2p states in the nanocluster. The electronic properties of the stereochemical lone pair in oxides such as SnO have been reviewed recently[50] We therefore propose that the modification of anatase with SnO nanoclusters will cause a reduction of the original TiO_2 band gap due to the presence of $(SnO)_x$ states at TiO_2 valence band, which pushes the valence band edge up in energy. Furthermore, an enhancement of charge (electron and hole) separation after photoexcitation is also expected by virtue of the nature of the valence and conduction band edges of the SnO-modified TiO_2 and we examine this point below.

In the analysis from the density of states, we consider simple Kohn-Sham energy eigenvalue differences, which can only give an indication that the surface modification of TiO_2 with SnO nanoclusters will reduce the band gap of TiO_2. In order to examine this in more detail, we have computed the optical absorption spectrum of a representative tin oxide nanocluster modified anatase heterostructure, namely $(SnO)_4$-modified anatase (001), since the PEDOS analysis above indicates that this structure will reduce the energy gap of anatase.

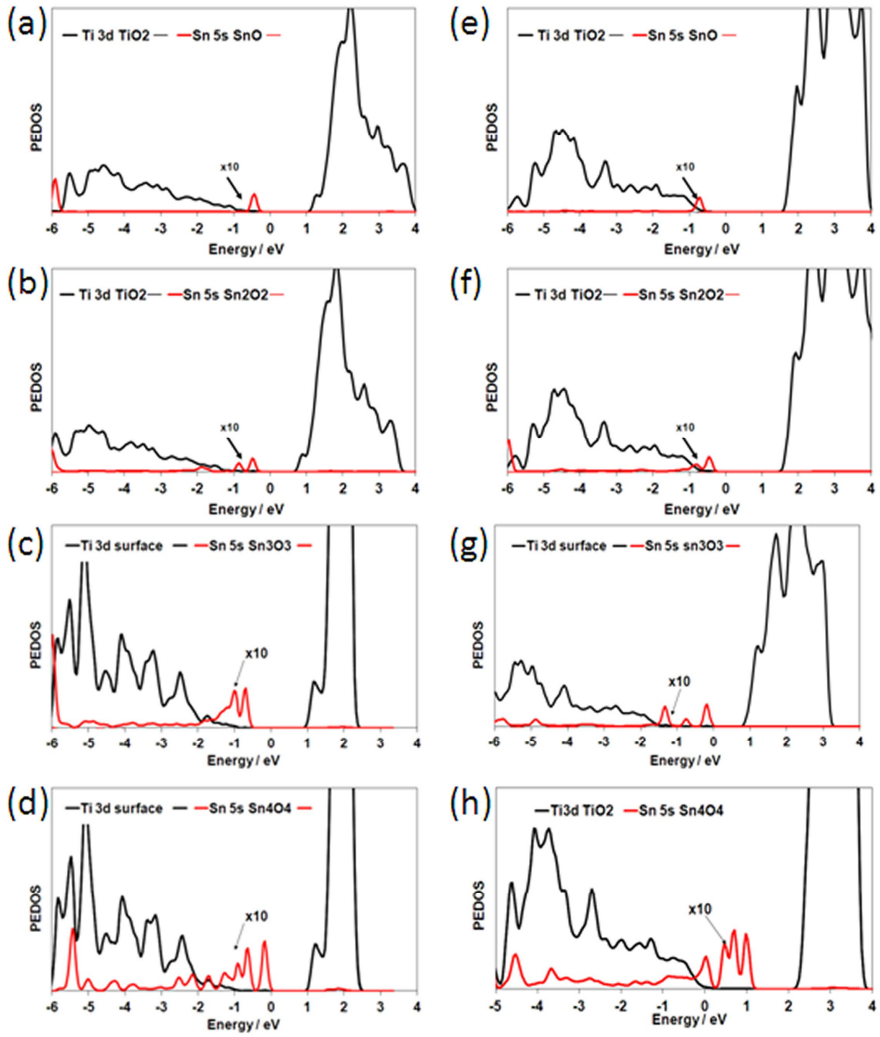

Fig. 2 Electronic density of states projected (PEDOS) onto Sn 5s, Ti 3d and O 2p (from the nanoclusters and the surface) states for (a) SnO, (b) Sn_2O_2, (d) Sn_3O_3, (e) Sn_4O_4, clusters supported on TiO_2 anatase (001) surface.

3.3. Modelling Photoexcitation in SnO-Modified Anatase

In the PEDOS plots of figure 2 we see that the top of the valence band is dominated by SnO derived states that arise from the lone pair in SnO, while the surface Ti 3d states dominate the bottom of the CB. This arrangement of valence and conduction band edges indicates separation of electrons and holes onto the surface and the nanocluster, respectively, upon photoexcitation. To examine charge separation we model the photoexcited state, as described in Section 2. It has recently been shown that this is a useful model system to study photoexcited anatase and rutile TiO_2[51,52] and has been applied in bulk HfO_2[53] and in rutile (110) modified with Ga_2O_3 and MgO nanoclusters[45]. For TiO_2 refs. 45, 50, 51 have shown that this model produces a localised Ti^{3+} electronic state in bulk anatase and the (101) surface[51], in rutile (110)[45,52] and in modified rutile (110)[45] (from hybrid DFT and DFT+U calculations). A localised oxygen hole state was also found with hybrid DFT[51] and with a +U correction on the O 2p states (to localise the valence band derived electronic hole after photoexcitation)[45]. Without a Hubbard U correction on the O 2p states, as in ref. 52 an incorrectly delocalised VB hole is found.

In all studies, singlet-triplet excitation energies have been calculated and relaxation (trapping) energies are presented in[45,51,53]. One finding from these investigations is that the excitation energy modelled in this fashion is always smaller than the simple VB-CB energy gap[45,51-53] since the latter does not account for relaxations after photoexcitation and the size of the relaxation energy can be significant. We emphasise again that this does not correspond to the energy that would be obtained from a TDDFT simulation of the photoexcited system, but nonetheless allows a useful examination of the electron and hole localisation.

Table 2 shows the singlet-triplet excitation, relaxation and vertical energies for the photoexcited state in $(SnO)_4$ modified anatase. The excitation, vertical and relaxation energies are defined in Section 2. In ref. 51 the anatase (101) singlet-triplet excitation energy from hybrid B3-LYP DFT is 3.25eV, which is smaller than the simple valence-conduction band energy gap. Similarly, in ref 45, where the same DFT+U set-up as

this paper is used, the singlet-triplet excitation energy of the bare rutile (110) surface was 1.69 eV, again smaller than the simple valence-conduction band energy gap.

Table 2: Singlet-triplet excitation and relaxation energies for the triplet excited state in SnO- modified TiO_2 in eV. Also shown are the same energies for the bare anatase (001) surface.

Structure	E^{S-T} / eV	E^{relax} / eV	$E^{vertical}$ / eV
SnO-TiO_2	0.50	0.96	1.46
Anatase TiO_2 (001)	1.11	1.26	2.37

The bare anatase (001) surface has a vertical energy of 2.37 eV, which is larger than rutile (2.1 eV). However, the singlet-triplet excitation energy shows a different behaviour: for anatase (001) it is 1.11 eV which is smaller than in rutile (110). We attribute this to the two surfaces having different relaxation energies – the relaxation energy of the anatase (001) surface, 1.26 eV, is notably larger than the value of 0.52 eV for the rutile (110) surface in ref. 45.

For $(SnO)_4$-modified anatase (001) the vertical energy in table 2, 1.46 eV, is consistent with the VB-CB energy gap and is smaller when compared to bare anatase. The singlet-triplet excitation energy is 0.5 eV, which is significantly reduced over the bare anatase singlet-triplet excitation energy. While the excitation energy from this model is smaller than the simple VB-CB energy gap[45,51-53] and the DFT energy gap underestimation persists, these results nonetheless confirm that modification of anatase with SnO nanocluster will have a positive impact on the light absorption characteristics of TiO_2 by reducing the excitation energy and bringing it into the visible region.

For photocatalytic efficiency, the fate of the electron and hole produced after photoexcitation is of crucial importance and is generally neglected in first principles studies of photocatalyst materials. Here we study the location of the electron and hole after photoexcitation, comparing with the bare anatase surface to make some conclusions on the effect of surface modification on the photocatalytic efficiency. The positions of the electron and hole produced after photoexcitation can be determined from the excess spin density, which is plotted for bare anatase (001) in figure 3(b). The spin density shows that the valence band derived hole is localised on a two-fold coordinated surface oxygen atom, which the electron is localised on a subsurface Ti site, giving localised Ti^{3+} and O^- (oxygen hole) species that are quite close to each other, similar to the (101) surface[52].

Figure 3 (a) shows the spin density of the relaxed triplet state for Sn_4O4-anatase, which allows us to examine the location of the electron and hole after photoexcitation. The electron is clearly localised on a Ti site in the surface layer of the anatase surface, which is assigned as a Ti^{3+} site. This is further confirmed by a computed Bader charge[54] of 1.68 electrons and a computed spin magnetisation of 0.97 electrons, while a Ti^{4+} cation has a computed Bader charge of 1.27 electrons and zero spin magnetisation. The localisation of the electron at this Ti site results in an elongation of Ti-O bonds of ca 0.1 Å, which is typical for Ti^{3+}-O distances compared to the Ti^{4+}-O distance.

The nature of the hole state is interesting. The spin density plot in figure 3 indicates that the hole is localised on two Sn-O bonds on the $(SnO)_4$ nanocluster, which is consistent with the composition of the valence band edge, namely that it is derived from the Sn(II)-O lone-pair interaction. These Sn ions have computed Bader charges of +1.67 and +1.65 electrons; by comparison, the computed Bader charge for Sn^{2+} in SnO is 1.84 electrons and the Bader charge of an Sn^{4+} cation in SnO_2 is *ca.* 0.2 electrons[30], from which we can assign a 3+ oxidation state to Sn in this photoexcited structure. We emphasise that the localisation of the hole is strong and the position of electron and hole indicate that the charge separation will be enhanced compared to bare anatase (001) and this will reduce charge recombination, which will manifest as a reduction in the PL peak associated with electron-hole recombination in anatase at 540nm[28]. Improved spatial charge separation will impact positively on the overall photocatalytic properties. The geometry around the hole site shows some changes compared to the singlet ground state structure, with Sn-O distances of 1.98 Å and 2.07 Å in the excited structures compared to 2.0 Å and 2.13 Å in the ground state, as shown in figure 3 (a).

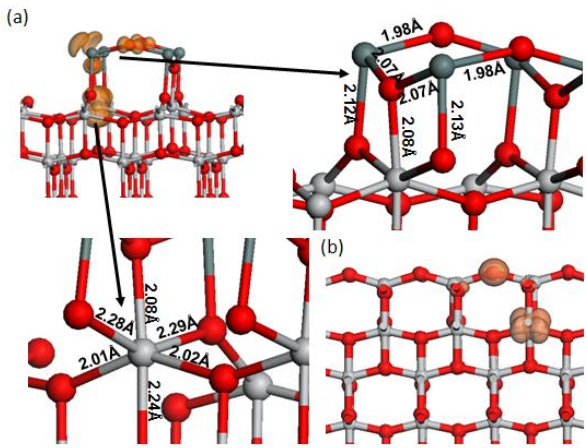

Fig.3 Computed excess spin density (isosurface values of 0.03 electrons/Å^3) and local geometry around the hole and electron sites in (a) Sn_4O_4-TiO_2 anatase (001) and (b) the unmodified anatase (001) surface from the relaxed triplet excited state model

4 Discussion

The results in this paper of a new approach to modifying anatase TiO_2 for visible light activated photocatalyst design, namely modification of anatase with Sn(II)O nanoclusters, highlight some interesting findings with respect to the twin activities of inducing visible light activity and reducing charge recombination in TiO_2 for photocatalysis.

In general, the findings for Sn(II)O modified TiO_2 are consistent with our previous findings from both experiment and theory for TiO_2 modified with nanoclusters of, e.g. TiO_2 [55,56], FeO_x[23,28], Ga_2O_3[39] and NiO[57] nanocluster modified TiO_2 and show some interesting contrasts towards fully oxidised Sn(IV)O_2-modified anatase[30]. In experimental work, the X-ray photoelectron spectra of FeO_x and NiO modified TiO_2 show a rise in the valance band (VB) due to TiO_2 surface modification[28,57], which is consistent with the band gap

reduction found in these structures.

The DFT results show that the valence band edge is shifted upwards, reducing the band gap compared to unmodified TiO_2 and this result is found from a DOS analysis, calculation of the optical absorption spectrum and an analysis of the photoexcited state. The latter also gives insights into the potential for enhanced electron-hole separation upon photoexcitation.

However, the materials composition considered in this work shows a novel way to induce both band gap reduction and charge separation by exploiting the presence of the lone-pair in nanoclusters of Sn(II)O that present at the top of the valence band, rather than the highly localised O 2p states in other oxides. It is the presence of these states that results in the upwards shift of the valence band edge and the separation of electrons and holes onto the surface and the nanocluster. When compared with bare TiO_2 surfaces and TiO_2 modified with other metal oxides, e.g. in ref. 45, where the hole is found on a single O atom in the nanocluster arising from the O 2p dominated valence band of these oxides. The difference in Sn(II)O-modified TiO_2, is associated with the presence of the Sn lone pair feature in Sn^{2+}[46,50], which means that the hole will have Sn 5s character with some contribution from oxygen nearest the Sn atoms.

An interesting contrast arises when comparing Sn(II)O modified anatase with $Sn(IV)O_2$ modified anatase[30], with no Sn-derived lone pair in the latter. In addition, the results of ref. 31 are also worth bringing into the discussion, in which these authors modified $ZnGa_2O_4$ with SnO_2 or SnO by simply using precursors with the desired Sn oxidation state. In these examples, the oxidation state of Sn played a determining role in the photocatalytic properties – modifying $ZnGa_2O_4$ with SnO species gives a band gap reduction, but modification with SnO_2 does not change the band gap. The origin of this difference is not developed in ref. 31, but the present results allow us to understand these findings. The presence of the Sn(II) lone pair states causes an upwards shift in the valence band edge relative to the parent oxide, which is not possible when using SnO_2, with no lone pair, as a surface modifier.

This raises the interesting possibility of exploiting the different electronic features of the oxidation states taken by metals which display a lone pair, such as Sn or Pb, to tune the photocatalytic properties of metal oxide nanocluster modified photocatalysts.

5. Conclusions

We present DFT simulations of a novel photocatalyst material, namely Sn(II)O nanoclusters supported on TiO_2 anatase (001) and show that the presence of the Sn(II)-O lone pair in the nanoclusters gives a new approach to engineering the key properties for photocatalysis. The key findings are that Sn(II)O modification of the anatase (001) surface will reduce the band gap over unmodified anatase, which will activate the catalyst in the visible region. This arises from the upwards shift of the valence band, which comes from the presence of the Sn 5s-O 2p lone pair in the nanocluster Enhanced charge separation, which is key for photocatalytic efficiency, arises from the separation of electrons and holes onto the anatase surface and the Sn(II)O nanocluster. Thus Sn(II)O nanocluster modified TiO_2 anatase is predicted to show improved photocatalytic properties over pure TiO_2.

Acknowledgements

We acknowledge support from Science Foundation Ireland (SFI) through the Starting Investigator Research Grant Program, project "EMOIN", grant number SFI 09/SIRG/I1620, and computing resources at Tyndall provided by SFI and by the SFI and Higher Education Authority funded Irish Centre for High End Computing. We acknowledge support from the European Union through the COST Action CM1104 "Reducible Oxide Chemistry, Structure and Functions".

Notes and references

Tyndall National Institute, University College Cork, Lee Maltings, Cork, Ireland
E-mail: michael.nolan@tyndall.ie

1 M. Ni, M. Leung, D. Leung, and K. Sumathy, K. *Renew. Sust. Energ. Rev.* 2007, **11**, 401 - 425
2 A. Fujishima, X. Zhang, and D. A. Tryk, *Surf. Sci. Rep*. 2008, **63**, 515 - 582
3 J. Zhao, C. Chen, and W. Ma, *Top. Catal.* 2005, **35**, 269 - 278
4 H. Choi, M. G. Antoniou, M. Pelaez, A. Delacruz, J. Shoemaker, and D. D. Dionysiou, *Environ. Sci. Technol.* 2007, **41**, 7530 - 7535
5 H. Yu, H. Irie, Y. Shimodaira, Y. Hosogi, Y. Kuroda, M. Miyauchi, and K. Hashimoto, K. *J. Phys. Chem. C*, 2010, **114**, 16481 - 16487
6 X. L. Nie, S. P. Zhou, G. Maeng, and K. Sohlberg, *Int. J. Photoenergy* 2009, 294042.
7 J. Nowotny, *Energy Environ. Sci*. 2008, **2**, 565 - 572
8 J. W. Zheng, A. Bhattcahrayya, P. Wu, Z. Chen, J. Highfield, Z. L. Dong, and R. Xu, *J. Phys. Chem. C* 2010, **114**, 7063 - 7069
9 C. Di Valentin, E. Finazzi, G. Pacchioni, A. Selloni, S. Livarghi, M. C. Paganini, and E. Giamello, E. *Chem. Phys*, 2007, **339**, 44 - 56
10 L. Bian, M. X. Song, T. L. Zhou, X. Y. Zhao, and Q. Q. Dai, *J. Rare Earths* 2009, **27**, 461 - 468.
11 R. Long, N. J. English, *J. Phys. Chem. C* 2010, **114**, 11984 - 11990
12 Y. Cui, H. H. Du, and L. S. Wen, *J. Mat. Sci. and Tech.* 2008, **24**, 675 - 689
13 A. Iwaszuk, and M. Nolan, M. *J. Phys. Chem. C,* 2011, ***115***, 12995 - 13007
14 J. G. Yu, Q. J. Xiang, M. H. Zhou, and X. Y. Zhou, *Appl Cat. B Environmental*, 2009, **90**, 595 - 602
15 M. Liu, L. Piao, L. Zhao, S. Ju, Z. Yan, T. He, C. Zhou, and W. Wang, *Chem. Commun.*, 2010, **46**, 1664 - 1666.
16 L. Gu, J. Wang, H. Cheng, Y. Du, and X. Han, *Chem. Comm.,* 2012, **48**, 6978 - 6980
17 W. Yang, J. Li, Y. Wang, F. Zhu, W. Shi, F. Wan, and D. Xu, *Chem. Commun*., 2011, **47**, 1809 - 1811.
18 Y. Q. Gai, J. B. Li, S. S. Li, J. B. Xia, and S. H. Wei, *Phys. Rev. Lett.* 2009, **102**, 036402/1 - 036402/4
19 H. G. Yang, C. H. Sun, S. Z. Qiao, J. Zou, G. Liu, S. C. Smith, H. M. Cheng, and G. Q. Lu, G. Q. *Nature,* 2008, **453**, 638 - 641
20 J. M. Herrmann, *New. J. Chem.,* 2012, **36**, 883 - 890
21 N. Murakami, T. Chiyoya, T. Tsubota, and T. Ohno, *Appl. Catal. A* 2008, **348**, 148 - 152
22 Fujishima, M.; Jin, Q.; Yamamoto, H.; Tada, H.; Nolan, M. *Phys. Chem. Chem. Phys.,* 2012, **14**, 705 - 711
23 M. Nolan, *Phys. Chem. Chem. Phys.*, 2011, **13**, 18194 - 18199
24 J. Libera, J. Elam, N. Sather, T. Rajh, and N. M. Dimitrijevic, *Chem. Mater.,* 2010, **22**, 409

25 L. Kong, Z. Jiang, T. Xiao, L. Lu, M. Jones, and P. P. Edwards, *Chem. Commun.,* 2011, **47**, 5512
26 H. Cheng, B. Huang, Y. Dai, X. Qin and X. Zhang, *Langmuir,* 2010, **26**, 6618
27 S. Hong, S. Lee, J. Jang and J. Lee, *Energy Environ. Sci*., 2011, **4**, 1781
28 H. Tada, Q. Jin, H. Nishijima, H. Yamamoto, M. Fujishima, S-i. Okuoka, T. Hattori, Y. Sumida, and H. Kobayashi, *Angew. Chem. Int. Ed*. 2011, **50**, 3501.
29 Q. Jin, M. Fujishima, and H. Tada, *J. Phys. Chem C*, 2011, **115**, 6478
30 Q. Jin, M. Fujishima, M. Nolan, A. Iwaszuk and H. Tada*, J. Phys. Chem. C,* 2012, **116***,* 12631
31 V. B. R. Boppana, and R. F. Lobo, *ACS Catal.,* 2011, **1**, 923
32 G. Kresse and J. Hafner, *Phys. Rev. B*, 1994, **49**, 1425.
33. Kresse G.; Furthmueller, J. *Comp. Mat. Sci.,* 1996, *6,* 15 - 50.
34. P. E. Blöchl, *Phys. Rev. B,* 1994, **50**, 17953.
35 J. P. Perdew, in Electronic Structure of Solids '91, ed. P. Ziesche and H. Eschrig, Akademie Verlag, Berlin, 1991.
36 B. J. Morgan, and G. W. Watson, *Surf. Sci*., 2007, **601**, 5034
37 M. Nolan, S. Grigoleit, D. C. Sayle, S. C. Parker and G. W. Watson, *Surf. Sci.* 2005, **576**, 217 - 229.
38 M. Lazzeri, and A. Selloni, *Phys. Rev. Lett.,* 2001, **87**, 266105/1 - 266105/4
39 E. Escamilla-Roaa, V. Timónb and A. Hernández-Laguna, *Computational and Theoretical Chemistry,* 2012, **981,** 59
40 R. Erdogana, O. Ozbeka and I. Onal, *Surf. Sci.,* 2010, **604,** 1029
41 M. Calatayud and C. Minot, *Surf. Sci.,* 2004, **552,** 169
42 M. Nolan, and G. W. Watson, *J. Chem. Phys.,* 2006, **125**, 144701/1 – 144701/6
43 B. J. Morgan, and G. W. Watson, *Phys. Rev. B* 2009, **80**, 233102/1 – 233102/4
44 P. R. Keating, D. O. Scanlon, B. J. Morgan, N. M. Galea, and G. W. Watson, *J. Phys. Chem. C,* 2012, **116**, 2443 - 2452
45 M. Nolan, *ACS Appl. Mater. Interfaces*, 2012, **4**, 5386 - 5393
46 A. Walsh and G. W. Watson, *Phys. Rev. B*, 2004, **70**, 235114/1 – 235114/7
47 L. A. Burton, and A. Walsh, *J. Solid State Chemistry,* 2012, **196**, 157 - 160.
48 A. A. Al-Sunaidi, A. A. Sokol, C. R. A. Catlow and S. M. Woodley, *J. Phys. Chem. C,* 2008, **112**, 18860 – 18865
49 C. R. A. Catlow, S. T. Bromley, S. Hamad, M. Mora-Fonz, A. A. Sokol and S. M. Woodley, *Phys Chem Chem Phys* 2010, **12**, 786
50 A. Walsh, D. J. Payne, R. G. Egdell and G. W. Watson, *Chem. Soc. Rev.,* 2011, **40**, 4455
51. C. Di Valentin and A. Selloni, *J. Phys. Chem. Lett.* 2011, **2**, 2223 - 2228
52 A. Jedidi, A. Markovits, C. Minot, S. Bouzriba and M. Abderraba,. *Langmuir*, 2010, **26**, 16232 - 16238
53 D. Munoz Ramo, P. V. Sushko and A. L. Shluger, *Phys. Rev. B*, 2012, **85**, 024120/1 – 024120/10
54 G. Henkelman, A. Arnaldsson, and H. Jónsson, *Comput. Mater. Sci.,* 2006, **36**, 354 - 360
55 A. Iwaszuk, and M. Nolan, *Phys. Chem. Chem. Phys*. 2011, **13**, 4963 - 4973
56 A. Iwaszuk, P. A. Mulheran, and M. Nolan, *J. Mat. Chem. A,* 2013, **1**, 2515 - 2525
57 Q. Jin, T. Ikeda, M. Fujishima, H. Tada, *Chem. Commun*. 2011, **47**, 8814 - 816

Graphical Abstract

Simulations demonstrate a new concept in designing photocatalyst materials based on TiO_2 modified with SnO, exploiting the Sn(II)-O lone pair to induce visible light absorption and charge carrier separation.